



6-1-2007

## Micelles of Different Morphologies - Advantages of Worm-like Filomicelles of PEO-PCL in Paclitaxel Delivery

Shenshen Cai  
*University of Pennsylvania*

Kandaswamy Vijayan  
*University of Pennsylvania*

Debbie Cheng  
*University of Pennsylvania*

Eliana M. Lima  
*University of Pennsylvania*

Dennis E. Discher  
*University of Pennsylvania*, [discher@seas.upenn.edu](mailto:discher@seas.upenn.edu)

Follow this and additional works at: [https://repository.upenn.edu/cbe\\_papers](https://repository.upenn.edu/cbe_papers)

 Part of the [Biochemical and Biomolecular Engineering Commons](#)

---

### Recommended Citation

Cai, S., Vijayan, ., Cheng, D., Lima, E. M., & Discher, D. E. (2007). Micelles of Different Morphologies - Advantages of Worm-like Filomicelles of PEO-PCL in Paclitaxel Delivery. Retrieved from [https://repository.upenn.edu/cbe\\_papers/91](https://repository.upenn.edu/cbe_papers/91)

Preprint version. Published in *Pharmaceutical Research*, Volume 24, Issue 6, June 2007, 14 pages.  
Publisher URL: 10.1007/s11095-007-9335-z

This paper is posted at ScholarlyCommons. [https://repository.upenn.edu/cbe\\_papers/91](https://repository.upenn.edu/cbe_papers/91)  
For more information, please contact [repository@pobox.upenn.edu](mailto:repository@pobox.upenn.edu).

---

## Micelles of Different Morphologies - Advantages of Worm-like Filomicelles of PEO-PCL in Paclitaxel Delivery

### Abstract

Worm-like and spherical micelles are both prepared here from the same amphiphilic diblock copolymer, poly(ethylene oxide)-*b*-poly( $\epsilon$ -caprolactone) (PEO [5 kDa]-PCL [6.5 kDa]) in order to compare loading and delivery of hydrophobic drugs. Worm-like micelles of this degradable copolymer are nanometers in cross-section and spontaneously assemble to stable lengths of microns, resembling filoviruses in some respects and thus suggesting the moniker "filomicelles". The highly flexible worm-like micelles can also be sonicated to generate kinetically stable spherical micelles composed of the same copolymer. The fission process exploits the finding that the PCL cores are fluid, rather than glassy or crystalline, and core-loading of the hydrophobic anticancer drug delivery, paclitaxel (TAX) shows that the worm-like micelles load and solubilize twice as much drug as spherical micelles. In cytotoxicity tests that compare to the clinically prevalent solubilizer, Cremophor® EL, both micellar carriers are far less toxic, and both types of TAX-loaded micelles also show 5-fold greater anticancer activity on A549 human lung cancer cells. PEO-PCL based worm-like filomicelles appear to be promising pharmaceutical nanocarriers with improved solubilization efficiency and comparable stability to spherical micelles, as well as better safety and efficacy *in vitro* compared to the prevalent Cremophor® EL TAX formulation.

### Keywords

lung carcinoma cells, paclitaxel, poly(epsilon-caprolactone), poly(ethylene oxide), worm-like micelle

### Disciplines

Biochemical and Biomolecular Engineering

### Comments

Preprint version. Published in *Pharmaceutical Research*, Volume 24, Issue 6, June 2007, 14 pages.  
Publisher URL: 10.1007/s11095-007-9335-z

## Metadata of the article that will be visualized in OnlineFirst

1	Article Title	<b>Micelles of Different Morphologies—Advantages of Worm-like Filomicelles of PEO-PCL in Paclitaxel Delivery</b>	
2	Journal Name	Pharmaceutical Research	
3		Family Name	<b>Discher</b>
4		Particle	
5		Given Name	<b>Dennis E.</b>
6	Corresponding Author	Suffix	
7		Organization	University of Pennsylvania Philadelphia
8		Division	Department of Chemical and Biomolecular Engineering
9		Address	Pennsylvania 19104, USA
10		e-mail	discher@seas.upenn.edu
11		Family Name	<b>Cai</b>
12		Particle	
13		Given Name	<b>Shenshen</b>
14		Suffix	
15	Author	Organization	University of Pennsylvania Philadelphia
16		Division	Department of Chemical and Biomolecular Engineering
17		Address	Pennsylvania 19104, USA
18		e-mail	
19			Family Name
20		Particle	
21		Given Name	<b>Kandaswamy</b>
22		Suffix	
23	Author	Organization	University of Pennsylvania Philadelphia
24		Division	Department of Chemical and Biomolecular Engineering
25		Address	Pennsylvania 19104, USA
26		e-mail	
27			Family Name
28		Particle	
29		Given Name	<b>Debbie</b>
30		Suffix	
31	Author	Organization	University of Pennsylvania Philadelphia
32		Division	Department of Chemical and Biomolecular Engineering
33		Address	Pennsylvania 19104, USA
34		e-mail	
35			Family Name

		<b>Lima</b>
36	Particle	
37	Given Name	<b>Eliana M.</b>
38	Suffix	
39	Author	
	Organization	University of Pennsylvania Philadelphia
40	Division	Department of Chemical and Biomolecular Engineering
41	Address	Pennsylvania 19104, USA
42	e-mail	
43	Received	10 April 2007
44	Schedule	Revised
45	Accepted	2 May 2007
46	Abstract	<p>Worm-like and spherical micelles are both prepared here from the same amphiphilic diblock copolymer, poly(ethylene oxide)-<i>b</i>-poly(<math>\epsilon</math>-caprolactone) (PEO [5 kDa]-PCL [6.5 kDa]) in order to compare loading and delivery of hydrophobic drugs. Worm-like micelles of this degradable copolymer are nanometers in cross-section and spontaneously assemble to stable lengths of microns, resembling filoviruses in some respects and thus suggesting the moniker 'filomicelles'. The highly flexible worm-like micelles can also be sonicated to generate kinetically stable spherical micelles composed of the same copolymer. The fission process exploits the finding that the PCL cores are fluid, rather than glassy or crystalline, and core-loading of the hydrophobic anticancer drug delivery, paclitaxel (TAX) shows that the worm-like micelles load and solubilize twice as much drug as spherical micelles. In cytotoxicity tests that compare to the clinically prevalent solubilizer, Cremophor® EL, both micellar carriers are far less toxic, and both types of TAX-loaded micelles also show 5-fold greater anticancer activity on A549 human lung cancer cells. PEO-PCL based worm-like filomicelles appear to be promising pharmaceutical nanocarriers with improved solubilization efficiency and comparable stability to spherical micelles, as well as better safety and efficacy <i>in vitro</i> compared to the prevalent Cremophor® EL TAX formulation.</p>
47	Keywords separated by ' - '	lung carcinoma cells - paclitaxel - poly( $\epsilon$ -caprolactone) - poly(ethylene oxide) - worm-like micelle
48	Foot note information	

## Research Paper

1  
2 **Micelles of Different Morphologies—Advantages of Worm-like Filomicelles**  
3 **of PEO-PCL in Paclitaxel Delivery**4 **Shenshen Cai,<sup>1</sup> Kandaswamy Vijayan,<sup>1</sup> Debbie Cheng,<sup>1</sup> Eliana M. Lima,<sup>1</sup> and Dennis E. Discher<sup>1,2</sup>**5 *Received April 10, 2007; accepted May 2, 2007*

**Abstract.** Worm-like and spherical micelles are both prepared here from the same amphiphilic diblock copolymer, poly(ethylene oxide)-*b*-poly ( $\epsilon$ -caprolactone) (PEO [5 kDa]-PCL [6.5 kDa]) in order to compare loading and delivery of hydrophobic drugs. Worm-like micelles of this degradable copolymer are nanometers in cross-section and spontaneously assemble to stable lengths of microns, resembling filoviruses in some respects and thus suggesting the moniker 'filomicelles'. The highly flexible worm-like micelles can also be sonicated to generate kinetically stable spherical micelles composed of the same copolymer. The fission process exploits the finding that the PCL cores are fluid, rather than glassy or crystalline, and core-loading of the hydrophobic anticancer drug delivery, paclitaxel (TAX) shows that the worm-like micelles load and solubilize twice as much drug as spherical micelles. In cytotoxicity tests that compare to the clinically prevalent solubilizer, Cremophor® EL, both micellar carriers are far less toxic, and both types of TAX-loaded micelles also show 5-fold greater anticancer activity on A549 human lung cancer cells. PEO-PCL based worm-like filomicelles appear to be promising pharmaceutical nanocarriers with improved solubilization efficiency and comparable stability to spherical micelles, as well as better safety and efficacy *in vitro* compared to the prevalent Cremophor® EL TAX formulation.

**KEY WORDS:** lung carcinoma cells; paclitaxel; poly( $\epsilon$ -caprolactone); poly(ethylene oxide); worm-like micelle.

24 **INTRODUCTION**

25 Parenteral delivery of chemotherapeutics is a cornerstone  
26 of clinical cancer treatment, but many drugs are hydrophobic  
27 and require a solubilizing carrier. Such systems must load and  
28 stably retain anticancer drugs and must also have a means to  
29 release drugs into cells. Anticancer drug delivery systems have  
30 thus far included bioconjugates (1–3), nanoparticles (4,5),  
31 liposomes (6,7), polymersomes (8–10), and polymeric micelles  
32 composed of amphiphilic block copolymers (11,12), but all of  
33 the cited carriers are essentially spherical in shape. Long and  
34 flexible “worm-like” micelle carriers made from amphiphilic  
35 block copolymers are described here in terms of formulation  
36 and *in vitro* delivery, and the findings follow up on recent  
37 studies that demonstrate surprisingly persistent circulation and  
38 potent anti-tumor activity of worm-like micelles *in vivo* (13).

39 Paclitaxel (TAX) is a clinically prevalent anticancer agent  
40 used against a variety of solid tumors (14–17), and it works by  
41 stabilizing microtubules and inhibiting cytoskeleton-mediated  
42 processes such as mitosis (18). However, the extremely low  
43 water solubility of TAX at 0.3  $\mu\text{g}/\text{ml}$  (25°C) (18) or 3–4  $\mu\text{g}/\text{ml}$   
44 at 37°C (19) has motivated both covalent modifications to  
45 increase solubility (20) as well as loading into various types of  
46 carrier systems. As the most common emulsifying agent used

in the clinic to solubilize TAX, Cremophor® EL is a complex, 47  
viscous mixture composed primarily of hydrophobic glycer- 48  
olpolyoxyethylene ricinoleates, various fatty acid esters, and 49  
~50% ethanol (21,22), but clinical problems associated with 50  
Cremophor EL include low drug stability after dilution in 51  
aqueous medium (23) and severe, dose-limiting side effects 52  
such as hypersensitivity and cardiotoxicity (20,24,25). There is 53  
therefore a need for safer and more effective TAX delivery 54  
systems. 55

Amphiphilic diblock copolymers generally self-assemble 56  
in dilute aqueous solution into three basic morphologies: 57  
spherical micelles, worm-like micelles, and vesicles. Spherical 58  
micelles form spontaneously when the hydrophilic, corona 59  
block such as poly(ethylene oxide) (PEO) is the largest block 60  
by mass, and these have now been widely studied in bio- 61  
application. Following parental administration, such spheres 62  
delay clearance by macrophages of the liver and spleen due 63  
to the hydrated corona and also—it has been thought—due 64  
to their small size (26). Escape from clearance in principle 65  
allows accumulation in tumors, and use of copolymers that 66  
are degradable (27,28) or sensitive to temperature or pH can 67  
provide mechanisms for controlled drug release (18,24,29). 68  
By decreasing the weight fraction of the PEO block to just 69  
less than ~50%, hydration and swelling of the corona imparts 70  
just enough curvature to the copolymer assembly that worm- 71  
like micelles that are microns in length and similar in 72  
diameter to the spheres are the predominant morphology 73  
for a variety of diblock copolymers (30,31). Drugs such as 74  
TAX and various hydrophobic dyes have now been loaded 75

<sup>1</sup>Department of Chemical and Biomolecular Engineering, University of Pennsylvania Philadelphia, Pennsylvania, 19104, USA.

<sup>2</sup>To whom correspondence should be addressed. (e-mail: discher@seas.upenn.edu)

76 into these novel carriers (30,32–34), and worm-like micelles  
 77 *in vivo* persist for up to 1 week in the blood circulation,  
 78 which appears longer than any other synthetic particle,  
 79 including stealthy vesicles bearing the same length of PEO  
 80 chains (13). In some sense, the worm-like micelles are bio-  
 81 inspired by filoviruses that can also circulate and infect  
 82 human cells, which is why the micelles are hereafter referred  
 83 to as filomicelles.

84 In this study, worm-like filomicelles and spherical  
 85 micelles were both prepared from the same poly (ethylene  
 86 oxide)-*b*-poly ( $\epsilon$ -caprolactone) (PEO-PCL, denoted OCL) as

sketched in Fig. 1a. Drug loading capacities were then  
 directly compared, and show that approximately 2-fold  
 higher TAX loading is possible with worm-like filomicelles.  
 For both systems, TAX release is similarly enhanced at lower  
 pH, which is favorable as cancerous tissues are generally  
 associated with acidic environment (29,35). Compared to  
 Cremophor EL, both polymeric micelle carriers show signifi-  
 cantly less cytotoxicity and greater potency in delivering  
 TAX to human lung carcinoma A549 cells. OCL-based  
 worm-like filomicelles thus appear to be a promising new  
 system for drug delivery.

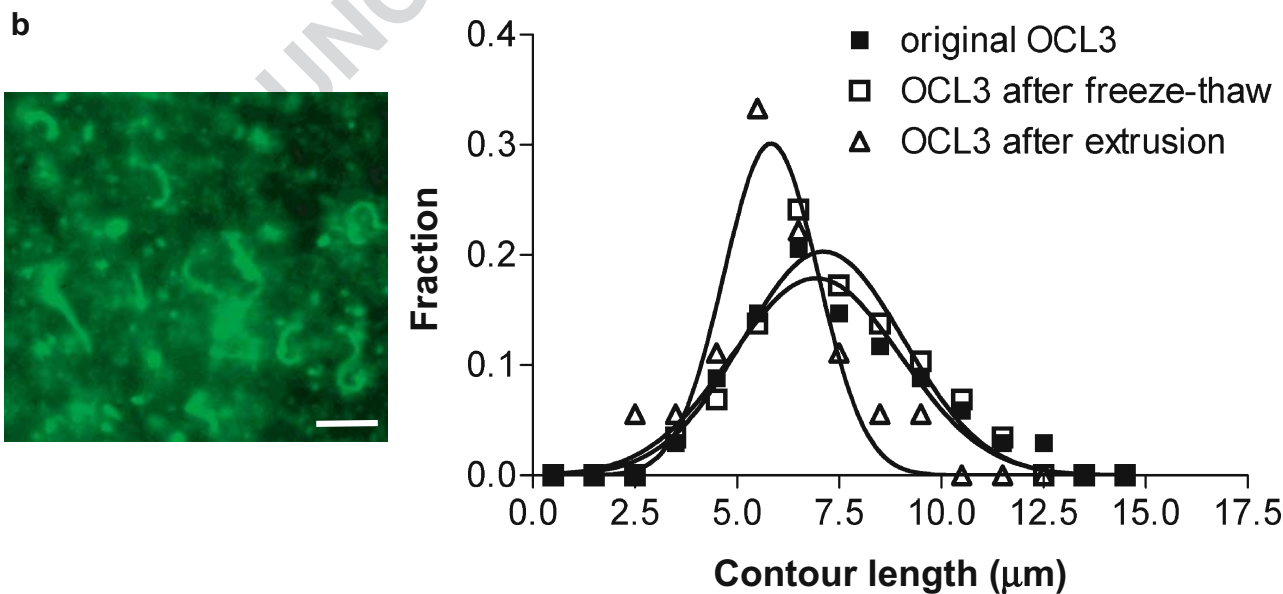
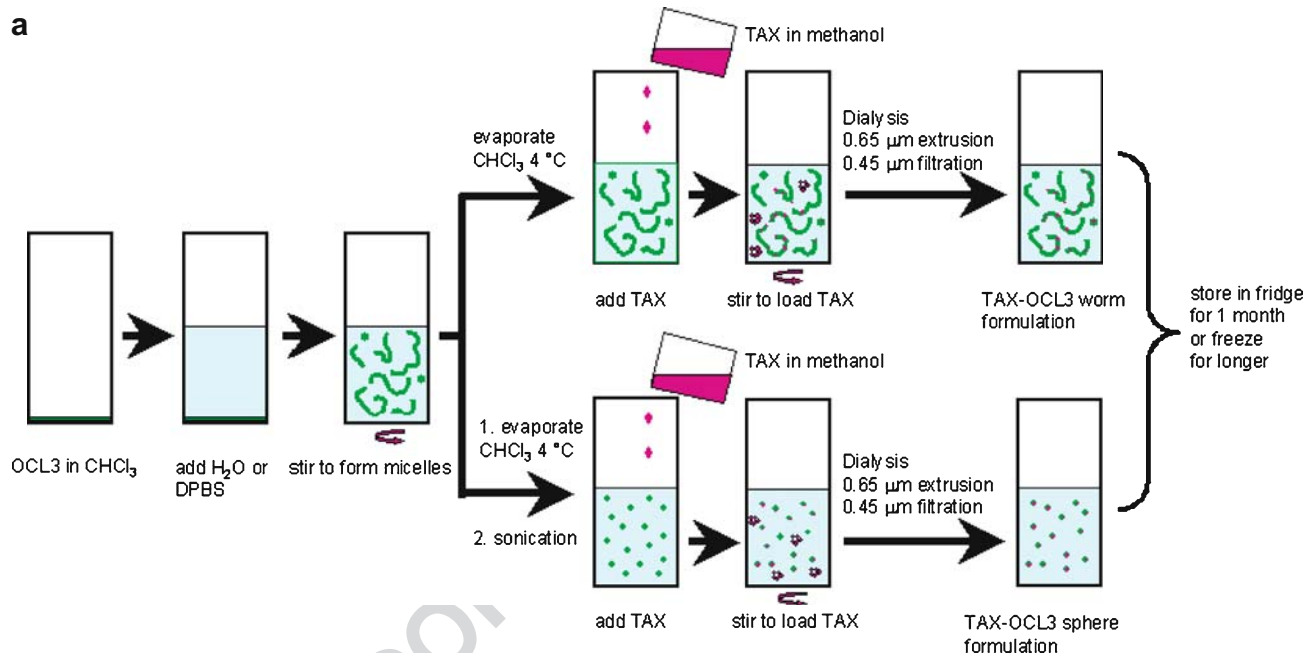


**Fig. 1.** Preparation of OCL3 polymeric micelles. **a** Scheme of making OCL3 micelles in worm-like and spherical morphologies; **b** visualization of worm-like micelles under fluorescence microscopy (left) and the contour length distribution of worm-like micelles, inset showing an enlarged worm-like micelle (right). Scale bar 5  $\mu$ m

**Micelles of Different Morphologies—Advantages of Worm-like Filomicelles of PEO-PCL in Paclitaxel Delivery**98 **MATERIALS AND METHODS**99 **Materials**

100 Diblock polymer poly (ethylene oxide)-*b*-poly ( $\epsilon$ -caprolactone)  
101 ( $M_n=5,000-6,500$ , weight fraction of PEO  $f_{EO}=0.43$ , polydispersity=  
102 1.3, denoted OCL3) was purchased from Polymersource  
103 (Dorval, Canada). Paclitaxel (TAX), docetaxel, Cremophor  
104 EL, fluorescent PKH26 dye, Dulbecco's phosphate-buffered  
105 saline (DPBS) and methylthiazolyldiphenyl-tetrazolium  
106 bromide (MTT) were from Sigma (St. Louis, MO). Human  
107 lung carcinoma cells A549 were obtained from ATCC  
108 (Manassas, VA). F12 Ham media was purchased from  
109 Mediatech (Herndon, VA). All organic solvents were  
110 analytical grade from Fisher Scientific.

111 **Preparation of OCL3 Polymeric Micelles by Cosolvent/  
112 Evaporation Method**

113 The preparation of OCL3 polymeric micelles was shown  
114 in Fig. 1a. Briefly, 50  $\mu$ l of 50 mg/ml OCL3 stock solution in  
115 chloroform was mixed with 5 ml of water and the mixture  
116 was stirred vigorously at room temperature for 1 h. Chloro-  
117 form was completely removed by evaporation at 4°C for  
118 overnight to obtain the final solution containing OCL3  
119 worm-like micelles. Solutions at other concentrations were  
120 made by varying the volume of OCL3 stock solution mixed  
121 with water. OCL3 spherical micelles were obtained by  
122 sonicating the worm-like micelles using Fisher 60 Sonic  
123 Dismembrator equipped with Fisher Ultrasonic Converter  
124 (Fisher Scientific) for 25 pulses at 1 s/pulse. All solutions  
125 containing OCL3 polymeric micelles were stored at 4°C to  
126 minimize degradation.

127 **Fluorescence Microscopy and Micelle Morphology Studies**

128 PKH26, which is a rhodamine-based hydrophobic fluores-  
129 cent dye, was added to OCL3 micelle solutions at about 1  $\mu$ l/1 mg  
130 polymer and vortexed for 10 s. The dye rapidly distributed into  
131 the hydrophobic core of the micelles so the morphology of  
132 micelles was visualized. Olympus IX71 inverted fluorescence  
133 microscope equipped with a 60 $\times$  objective lens and a Cascade  
134 CCD camera was used to observe the micelles. About 25  
135 images were taken for each sample tested and the contour  
136 length of worm-like micelles was measured using Image-Pro  
137 Plus (MediaCybernetics, Silver Spring, MD).

138 **Dynamic Light Scattering**

139 The average hydrodynamic micelle sizes and size distribution  
140 were analyzed by dynamic light scattering (DLS) using Protein  
141 Solutions™ Temperature Controlled MicroSampler and Protein  
142 Solutions Dynapro™ Titan (Wyatt Technologies, Santa Barbara,  
143 CA) at 25°C. The laser wavelength was 782.4 nm and the  
144 scattering angle was 90°. Each sample was measured in triplicate.

145 **Crystallinity Analysis**

146 Polycaprolactone is a highly crystalline polymer in bulk.  
147 In an attempt to look for crystallization at nano-scale, an  
148 alternate protocol was developed that could exploit the

melting and annealing of the PCL core. Thus a 10 mg/ml stock 149  
solution of OCL3 was prepared in chloroform and 15–20  $\mu$ l of 150  
this stock was added to 1 ml water in a glass vial. The vial was 151  
closed, briefly vortexed, and allowed to stand at room 152  
temperature for 2 h. Next, the vial was incubated at 60°C with 153  
the cap open, for 2 h to evaporate the chloroform in the 154  
solution. The vial was then allowed to incubate at 30°C for 4–6 h. 155  
Glycerol was added to the worms to make a 50% glycerol 156  
solution, which was incubated at –20°C for up to 24 h. The 157  
rigidity of OCL3 worms was determined by fluorescence image 158  
analysis as described in “Fluorescence Microscopy and Micelle 159  
Morphology Studies.” 160

The fluidity of the worm micelle core was estimated by 161  
measuring the fluorescence recovery after photobleaching 162  
(FRAP) of the PKH26 dye. Briefly, an aperture on the light 163  
path is used to selectively overexpose a small section of the 164  
worm. The fluorescence recovery in the bleached region is 165  
monitored by comparing the fluorescent intensity to that of 166  
the Intensity in an unbleached section of the worm. 167

**Paclitaxel (TAX) Encapsulation in OCL3 Micelles** 168

TAX of 50 mg/ml in methanol was added into the micelle 169  
solutions to obtain desired spiked TAX/polymer ratios. The 170  
mixture was stirred at 25°C for 20 min and transferred to dialysis 171  
cassettes (MWCO 10,000, Pierce, Rockford, IL). Dialysis was 172  
performed against DPBS (pH 7.4) for 2 h to remove methanol 173  
and small residues of dissolved TAX, and the obtained TAX- 174  
loaded micelles were separated from insoluble-free TAX aggre- 175  
gates by extrusion through a 10 ml thermobarrel extruder 176  
(Northern Lipids, Vancouver, Canada) fitted with 0.65  $\mu$ m 177  
filtering membranes (Millipore, Bedford, MA), and further 178  
purified by filtration through 0.45  $\mu$ m Fischerbrand MCE filter 179  
(Fisher Scientific). The preparation of TAX-encapsulated OCL3 180  
micelles is illustrated in Fig. 1a. As an alternative method, TAX 181  
was mixed with OCL3 polymer in chloroform solution before 182  
micelle formation. The TAX-loaded micelles were then 183  
obtained as described in “Preparation of OCL3 Polymeric 184  
Micelles by cosolvent/Evaporation Method” followed by dialy- 185  
sis and extrusion. 186

**HPLC Assay Development and Validation** 187

A Waters HPLC system (Waters, Milford, MA) equipped 188  
with a 1525 Binary HPLC pump, a symmetry® reverse-phase 189  
C<sub>18</sub> 5.0  $\mu$ m column (4.6 $\times$ 150 mm), and a 2487 Dual  $\lambda$  190  
absorbance UV detector was used for TAX quantification. A 191  
series of 1:2 TAX dilutions in acetonitrile ranging from 0 to 192  
0.25 mg/ml were pre-mixed with equal volume of 0.25 mg/ml 193  
docetaxel in acetonitrile as internal standard. The solutions 194  
were filtered through 0.45  $\mu$ m filter followed by injection into 195  
HPLC system. A mobile phase of 58% H<sub>2</sub>O, 42% acetonitrile 196  
at a flow rate of 1 ml/min was applied. TAX was detected and 197  
quantified at UV 220 nm. The standard curve by plotting the 198  
ratio of AUC of TAX and docetaxel was established, and the 199  
linear range, intra-day and inter-day coefficient of variance 200  
(CV), lower limit of detection (LLOD), lower limit of 201  
quantification (LLOQ), assay accuracy and recovery (by 202  
testing with 3, 10, and 40  $\mu$ g/ml TAX solution using the 203  
standard curve) were calculated. To use the validated HPLC 204  
assay to determine the TAX loading capacity and efficiency 205

206 in OCL3 micelles, TAX-loaded micelles were pre-mixed  
 207 with equal volume of 0.25 mg/ml docetaxel in acetonitrile,  
 208 and acetonitrile in equal volume to the mixture was further  
 209 added, followed by the HPLC analysis using the standard  
 210 curve described above. TAX loading capacity and efficiency  
 211 were calculated based on the following expressions:

$$\text{TAX loading capacity} = \frac{\text{mass of TAX encapsulated in micelles/}}{\text{mass of OCL3 polymeric micelles}}$$

$$\text{TAX loading efficiency} = \frac{\text{mass of TAX encapsulated in micelles/}}{\text{mass of initially added TAX}}$$

217 **Thermal Analysis**

218 Thermal tests of OCL3 micelles were performed by  
 219 differential scanning calorimetry (DSC) using a Differential  
 220 Scanning Calorimeter 2920 (TA instruments, New Castle, DE).

221 TAX-loaded OCL3 worm micelles were lyophilized  
 222 before the analysis. DSC thermograms of OCL3-TAX  
 223 mixture (either in bulk before TAX loading or in lyophilized  
 224 form after TAX loading) and OCL3 alone were then  
 225 obtained by heating in sealed standard aluminum pans (TA  
 226 instruments) from 25 to 100°C at a rate of 10°C/min followed  
 227 by air cool and reheating to 100°C at the same rate.

228 **Micelle Stability and Paclitaxel Release Studies**

229 Both worm-like and spherical micelles (10 mg/ml), either  
 230 drug-loaded or free, were stored at 4°C for 1 month or  
 231 subjected to one-time freeze-thawing cycle. Then, the  
 232 particle size was measured by DLS and the morphology was  
 233 tested by fluorescent microscopy. TAX-loaded micelles were  
 234 also examined for drug leakage potentially caused by storage  
 235 or freeze-thawing cycles by centrifugation at 3,000 rpm for 5  
 236 min to precipitate the TAX that may have diffused out. The  
 237 supernatant was then mixed with acetonitrile and internal  
 238 standard docetaxel for HPLC analysis.

239 Further, a dialysis method was employed to evaluate the  
 240 *in vitro* release of TAX from OCL3 micelles. TAX-loaded  
 241 worm-like and spherical micelles at a TAX concentration of  
 242 40 µg/ml were added to the dialysis cassettes and dialyzed at  
 243 37°C against DPBS of pH 6.8 and pH 7.4. At certain time  
 244 points, the release medium was sampled and fresh DPBS was  
 245 added to maintain the volume. The sampled medium was  
 246 lyophilized and redissolved in chloroform. The insoluble  
 247 buffer salt was removed by filtration. Chloroform was  
 248 evaporated then and the remaining sample was re-dissolved  
 249 in acetonitrile and subjected to aforementioned HPLC  
 250 analysis.

251 **Cytotoxicity Assay**

252 TAX-loaded and drug-free micelles at serial dilutions were  
 253 prepared per above. For comparison, 12 mg/ml TAX in ethanol  
 254 was mixed with equal volume of Cremophor® EL followed by  
 255 sonication for 30 min. The obtained Cremophor EL TAX was  
 256 diluted with DPBS to obtain desired TAX concentrations.

257 Human lung-derived carcinoma cells A549 were grown  
 258 in F12 Ham media supplemented with 10% fetal bovine  
 259 serum and 100 U/ml penicillin and 100 µg/ml streptomycin at

37°C, 5% CO<sub>2</sub> to 60–70% confluence. A549 cells (50,000 cell/ml) 260  
 were seeded in 96-well plates at 5,000 cells per well and 261  
 cultured for 24 h to allow attachment. The medium was then 262  
 exchanged and 100 µl of different tested formulations (free 263  
 worm-like and spherical OCL3 micelles, Cremophor EL, free 264  
 drug, TAX-loaded worm-like and spherical micelles, and 265  
 Cremophor EL TAX) was added. As control, 100 µl of DPBS 266  
 was added to cells not exposed to those formulations. After 267  
 37°C, 5% CO<sub>2</sub> incubation for 72 h, the media were discarded, 268  
 and 100 µl/well F12 Ham medium and 11 µl/well of 5 mg/ml 269  
 MTT solution in DPBS was added. The plates were incu- 270  
 bated at 37°C for 3 h and the media were removed again. The 271  
 intracellular metabolized product MTT formazan was re- 272  
 trieved by addition of 100 µl/well DMSO and incubation at 273  
 room temperature for 5 min. The plates were read at 550 nm, 274  
 and the cell viability was calculated as (reading of wells with 275  
 cells exposed to tested formulations—reading of blank wells)/ 276  
 (reading of wells with cells exposed to DPBS—reading of 277  
 blank wells). 278

279 **Data Analysis**

280 All data that require non-linear regression analysis were 280  
 processed using GraphPad Prism (Version 4.03, GraphPad 281  
 Software, San Diego, CA). The contour length distribution of 282  
 OCL3 worm-like micelles was fit by Gaussian distribution, 283  
 TAX and the carrier cytotoxicity assay on A549 cells was fit 284  
 by sigmoid dose-response curve equation. 285

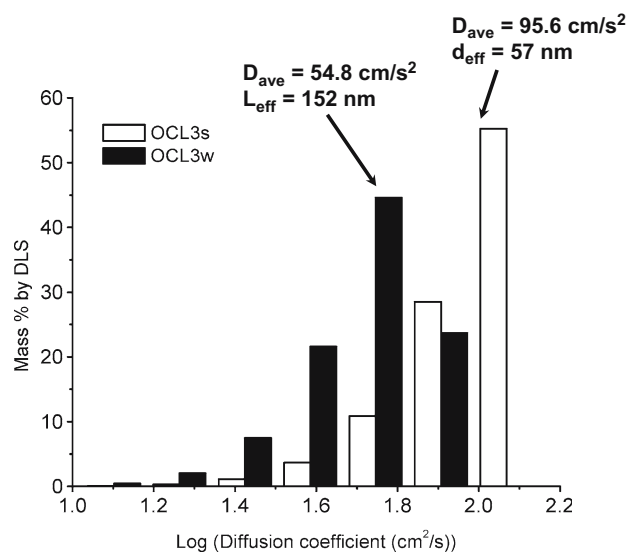


**Fig. 2.** Size and diffusion analysis of OCL3 micelles. The average diffusion coefficient distribution, and the calculated effective hydrodynamic size (diameter or length) of worm-like (before sonication) and spherical (after sonication) micelles were measured by DLS. The calculation of effective length of worm-like micelles is based on Stokes-Einstein equation:  $D = kT / (2\pi\eta L_{eff})$  for worms (43) and  $D = kT / (3\pi\eta d_{eff})$  for spheres, where  $D$  is the diffusion coefficient,  $k$  is the Boltzmann constant ( $1.38 \times 10^{-23}$  J/K),  $T$  is the temperature (25°C),  $\eta$  is the viscosity of the solution (1.02 mPa·s from DLS), and  $d_{eff}$  is the hydrodynamic radius multiplied by 2



**Micelles of Different Morphologies—Advantages of Worm-like Filomicelles of PEO-PCL in Paclitaxel Delivery**

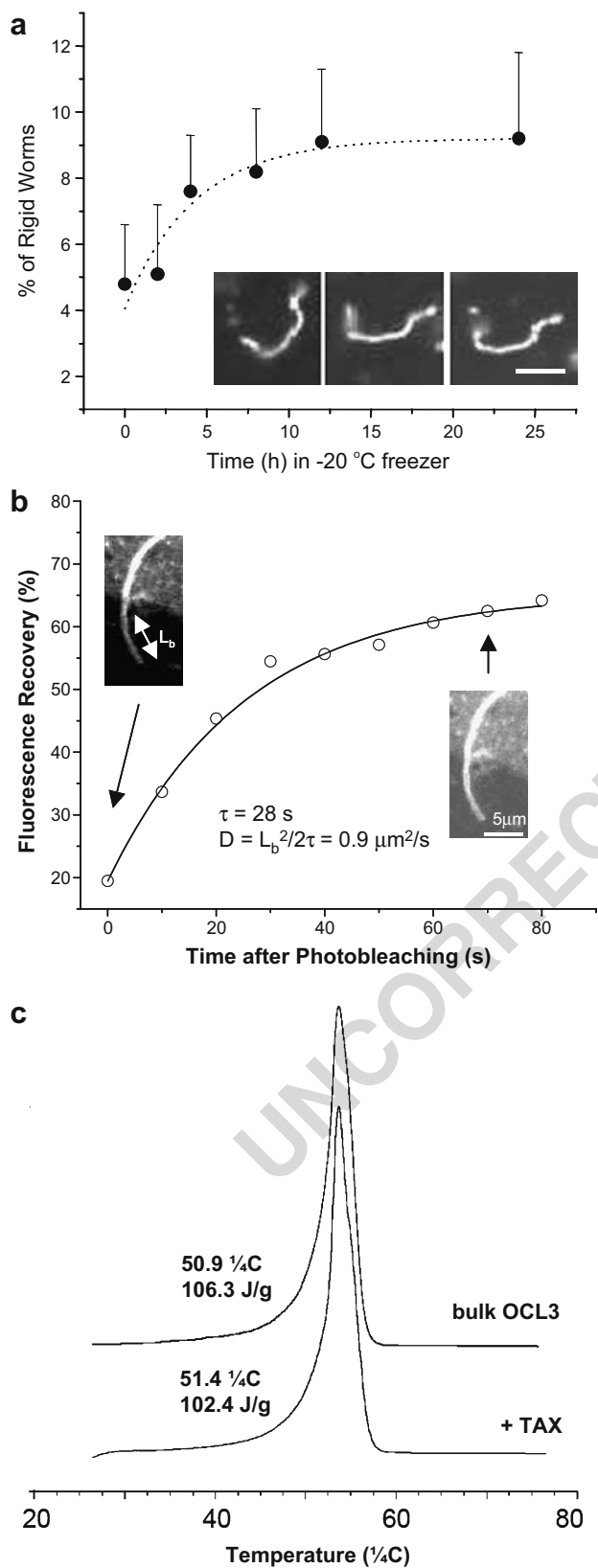


**Fig. 3.** Thermal and crystallinity analysis of OCL3 micelles. **a** Fluorescence recovery after photobleaching (FRAP) curve on OCL3 worms: A manual aperture in the light path was used to overexpose a small end section of the worm. The intensity in the bleached section was compared to that of a similar length of the worm in the unbleached section to normalize for bleaching during imaging. The FRAP data were fitted to an exponential recovery curve: Recovery % =  $A(1 - e^{-t/\tau})$  (where  $A$  is the maximum recovery percentage and  $t$  is the time for recovery) to obtain an average recovery time constant  $\tau \sim 28$  s. The 1-D diffusivity of the PKH26 dye was calculated from  $D = L_b^2/2\tau$  where  $L_b$  is the length of the bleached region, and  $\tau$  is the recovery time constant.  $D \sim 0.9 \mu\text{m}^2/\text{s}$ . **b** Percentage of rigid OCL3 worm-like micelles with possible crystallized cores over 12 h incubation at  $-20^\circ\text{C}$  either in a 50% glycerol solution or pure water, after heating to  $60^\circ\text{C}$  and cooling to  $30^\circ\text{C}$ . The inset figures show frames in several different time points from sample rigid worms that were formed in glycerol. Scale bar 5  $\mu\text{m}$ . **c** DSC thermogram ranging from 25 to  $80^\circ\text{C}$  of OCL3 polymer alone and TAX-OCL3 mixture

**RESULTS**

286

**OCL3 Filomicelles are Fluid and can Fission to Spheres**

287

A simple physicochemical measure of aggregate stability for strongly segregating amphiphiles is the critical micelle concentration (CMC), which is expected to be exponential in the length of the hydrophobic block (36). Based on a CMC of 1.2  $\mu\text{g}/\text{ml}$  for a sphere-forming OCL copolymer, EO<sub>44</sub>-CL<sub>21</sub> (37), we estimate an immeasurably small CMC for our OCL3 copolymer EO<sub>110</sub>-CL<sub>58</sub> of less than 1  $\text{fg}/\text{ml}$  (i.e.  $\text{CMC}_{\text{OCL3}} \sim [1.2 \mu\text{g}/\text{ml}]^{58/21}$ ). For later comparison, Cremophor EL reportedly has a  $\text{CMC}_{\text{CremEL}} \sim 90 \mu\text{g}/\text{ml}$ . For OCL3, micellar assemblies are clearly the predominant form in any aqueous solution. Moreover, since molecular exchange rates between micelles scale inversely with CMC, these low-CMC micelles can be considered kinetically trapped or frozen—without implying glassiness or crystallinity. OCL3’s weight fraction of  $\sim 0.43$  for the hydrophilic PEO block drives assembly of most of the copolymer into worm-like and flexible filomicelles as observed by fluorescence microscopy after adding hydrophobic fluorescent dyes (Fig. 1b, inset). The average contour length of spontaneously assembled OCL3 filomicelles was calculated from measurement of at least 50 filomicelles, and as shown in Fig. 1b, most of the filomicelles are 6–7  $\mu\text{m}$ , with some filomicelles as long as 14  $\mu\text{m}$ .

288

289

290

291

292

293

294

295

296

297

298

299

300

301

302

303

304

305

306

307

308

309

Extrusion of worm-like filomicelles at high pressures and flow rates through nanoporous filters has been used to controllably reduce their length (13), but in order to convert to spherical micelles—simply and quantitatively—we exposed the filomicelles to robust sonication for several minutes. Diffusion coefficients ( $D_{\text{ave}}$ ) were then measured by dynamic light scattering (DLS), and after sonication the effective hydrodynamic diameter was  $\sim 57$  nm (Fig. 2). This is similar to previous  $\sim 60$  nm estimates for the OCL3 filomicelle diameter of core plus corona as based on cryo-TEM (13). Prior to sonication, the measured  $D_{\text{ave}}$  proves significantly smaller and yields only a crude approximation for a larger effective size, but more important is the minimal overlap of the two distributions for  $D_{\text{ave}}$ . The 22% overlap suggests that a small fraction at most of the pre-sonicated

310

311

312

313

314

315

316

317

318

319

320

321

322

323

324

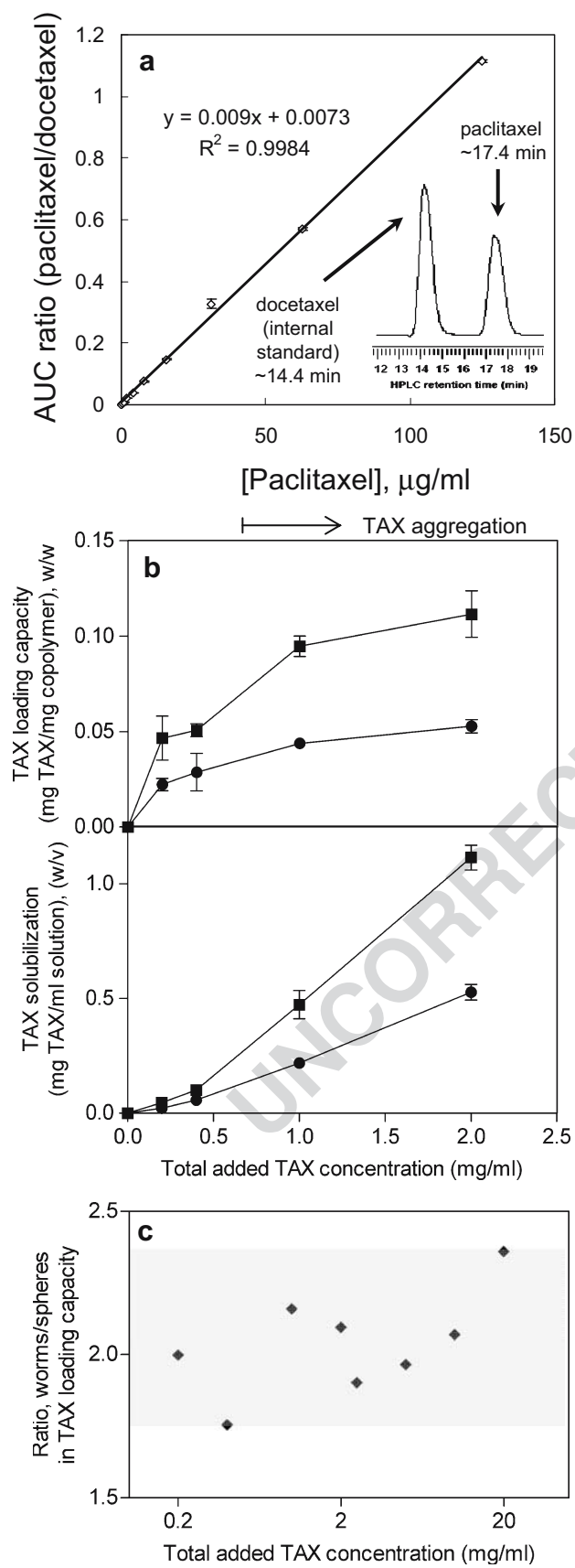


**Fig. 4.** HPLC-UV assay for paclitaxel (TAX) encapsulation. **a** Plot of HPLC-UV-determined area-under-curve (AUC) ratio between TAX and docetaxel vs TAX concentration. *Inset* shows the HPLC-UV spectrum of docetaxel (as internal standard) and paclitaxel (TAX). **b** TAX loading capacity (*upper panel*, defined as mg TAX loaded per milligram micelle) and solubilization (*lower panel*, defined as mg TAX loaded per milliliter aqueous solution) with OCL3 micelles when total added TAX:OCL3 micelle (w/w)=1:5; **c** ratio between TAX loading capacity with OCL3 worms and spheres at different conditions: Total added TAX:OCL3 micelle (w/w) was fixed at 1:5 while OCL3 concentration varied when added TAX concentration  $\leq 2$  mg/ml, and OCL3 micelle concentration was fixed at 10% (w/v) when added TAX concentration  $> 2$  mg/ml

sample consists of spherical micelles. Worm-like filomicelles therefore predominate in freshly prepared OCL3 samples.

In bulk, PCL is a crystalline polymer at room temperature with melting in the range of 40–60°C (38), but past studies of PEO-based diblock copolymers in bulk suggest that PEO crystallization dominates in the same temperature range and frustrates crystallization of the connected block (38). For example, the diblock PEO-polyethylene (PE) in bulk is 70% PEO and only 10% crystalline (PE). On the other hand, dilution of filomicelles into water will generally hydrate and dissolve any crystallinity in the PEO corona. We had previously reported that OCL filomicelles appear as flexible as worm-like micelles made from non-crystalline and non-glassy diblock copolymers (e.g. PEO-polybutadiene), which implies a fluid core of PCL (30,39). However, our interest in loading and storage here involved freezing for an extended time, which are conditions that favor crystallization.

A very small fraction of the OCL3 filomicelles are inflexible coils as identified by end-to-end fluctuation  $< 5\%$  of the average end-to-end distances relative to the more fluid-like and flexible filomicelles (Fig. 3a). Freezing in glycerol gave up to 10% of the bent but crystalline-behaving worm-like micelles (Fig. 3a). The core fluidity of the dominant population of flexible filomicelles was subsequently estimated by fluorescence recovery after photobleaching (FRAP) studies of immobilized filomicelles (Fig. 3b). The average recovery time for four different worms was  $\sim 30$  s, which is similar to that observed in PBD cores of worm-like micelles with a similar molecular weight (40). The fast recovery rate in FRAP and the minor percentage of rigid worm micelles indicate a highly fluid PCL core, which would tend to favor loading and retention of hydrophobic drugs such as paclitaxel (TAX). Fluidity also provides a basis for filomicelle flexibility, which might allow these long micelles to reptate into diseased tissues, including tumors, despite their micron-scale length.

Before examining TAX loading of filomicelles and spheres in dilute solution, we examined the bulk melting of OCL3 with or without TAX using differential scanning calorimetry (DSC). A melting onset temperature near 51°C (Fig. 3c) is consistent with PEO and/or PCL crystallization, and the finding that TAX exerted no significant effect on melting temperature indicates a relative absence of disruptive interactions between the drug and the copolymer. Assuming the melting is attributable predominantly to PEO crystallization, as cited above (41), we estimate PEO crystallinity of 81% from the measured endotherm peak area (106.3 J/g without TAX), the heat of fusion for pure PEO ( $\sim 300$  J/g) (41), and the  $f_{EO}$  of OCL3. With the presence of TAX, there

325  
326  
327  
328  
329  
330  
331  
332  
333  
334  
335  
336  
337  
338  
339  
340  
341  
342  
343  
344  
345  
346  
347  
348  
349  
350  
351  
352  
353  
354  
355  
356  
357  
358  
359  
360  
361  
362  
363  
364  
365  
366  
367  
368  
369  
370  
371  
372

**Micelles of Different Morphologies—Advantages of Worm-like Filomicelles of PEO-PCL in Paclitaxel Delivery**

**Table I.** Validation of HPLC-UV Assay for Paclitaxel, Using Docetaxel as the Internal Standard

	Values
t1.2	
t1.3	Linear range 0.5–125 µg/ml
t1.4	Intra-day CV <15%, max 12.3%
t1.5	Inter-day CV <15%, max 14.4%
t1.6	Baseline noise ~0.0001 AU
t1.7	LLOD 0.5 µg/ml
t1.8	LLOQ 1.0 µg/ml
t1.9	Accuracy 100.2±7.8%
t1.10	Recovery 101.7±6.1%

is no apparent decrease of crystalline PEO (79%) in bulk OCL3 (102.4 J/g with TAX), suggesting that TAX interaction with the copolymer is negligible.

**Paclitaxel Integration into OCL3 Spheres and Filaments**

TAX was then loaded into dilute micelles, and HPLC analysis was used to characterize the loading properties. An internal standard, docetaxel, was added in fixed amount to minimize variability (Fig. 4a; Table I). The lower limit of detection (LLOD) and lower limit of quantification (LLOQ) were as low as 0.5 and 1 µg/ml, and both the intra-day and inter-day coefficients of variance (CV) were less than 15%. An accuracy of 100.2±7.8% (n=6) and a recovery of 101.7±6.1% (n=6), were also obtained.

Loading of TAX before or after micelle formation showed no significant difference in capacity or efficiency (not shown). Figure 4b shows the TAX loading capacity and final concentration when TAX was initially added in a fixed 1:5 w/w ratio to micelles. Increasing TAX from 0.2 to 2 mg/ml (OCL3 1–10 mg/ml) increased both the loading capacity of TAX and the final solubilized TAX. Compared to spheres, OCL3 filomicelles showed about 2-fold greater loading capacity and at all concentrations (Fig. 4c).

Up to 10% w/v polymer concentration, with TAX varied from 2.5 to 5 mg/ml, the loading capacity for TAX increased, although the w/w loading was higher for 5% polymer. Further increases of added TAX up to 20 mg/ml led to a decrease in TAX solubilization regardless of morphology; this is probably due to the well-known aggregation of TAX at extremely high concentrations. The highest TAX solubilization obtained in the studies of filomicelles to date was 3 mg/ml, which is about 10,000-fold higher than natural TAX solubility in aqueous buffer [0.3 µg/ml, (18)]. Drug loading efficiency defined as (loaded drug/added drug) is

**Table III.** Loading Efficiency of TAX into OCL3 Spherical and Worm-like Micelles at 10% (w/v) Fixed OCL3 Micelle Concentration

	Total TAX Concentration (mg/ml)			
	2.5	5	10	20
Spheres	0.34	0.30	0.09	0.03
Worms	0.64	0.59	0.18	0.06

*Loading Efficiency* mass of solubilized TAX/mass of initially added TAX

tabulated in Tables II, III, and IV and consistently appears 2-fold higher with filomicelles than with spherical micelles.

In addition to the encapsulation capacity studies, an identical DSC thermogram for lyophilized OCL3–TAX mixture after encapsulation (not shown) with that of OCL3–TAX mixture in bulk (Fig. 3c) again verifies the unchanged melting temperature and the fusion heat of OCL3 copolymer. This further demonstrates the absence of interactions of TAX with its excipient during the encapsulation process.

**Stability and In Vitro Release**

Possible effects of storage, drug loading and extrusion on morphological changes of filomicelles were examined by DLS and fluorescence imaging. Fig. 5a shows that (1) both shapes of micelle are morphologically stable in 4°C storage for up to 1 month; (2) TAX integration does not affect micelle size, which is probably because the small loaded mass of TAX cannot swell the relatively large cores within micelles; (3) spherical micelles made by sonicating worm-like filomicelles show no further size change after extrusion whereas filomicelles become smaller. The latter result was confirmed by contour length measurement under fluorescence microscopy (Fig. 1b), which shows that extrusion left-shifts and narrows the length distribution from 6.6–7.3 µm (95%) to 5.6–6.1 µm.

Stability of TAX loading within OCL3 micelles was evaluated after 1 month of storage. Fig. 5b shows that when TAX-loaded micelles of either morphology were either maintained in fluid form at 4°C or else frozen (and perhaps crystalline) at –20°C, no significant leakage or precipitation of TAX could be detected. As emphasized above and further below, the filomicelle carriers are clearly stable under harsh treatments. For application, freezing has the advantage in slowing hydrolytic degradation of PCL (30).

In addition, filomicelles were subjected to freeze–thaw cycles (–20°C) as another potentially disruptive operation

**Table II.** Loading Efficiency of TAX into OCL3 Spherical and Worm-like Micelles When Initial Added TAX:OCL3 Micelle (w/w)=1:5

	Total TAX Concentration (mg/ml)				
	0.2	0.4	1	2	20
Spheres	0.11	0.14	0.22	0.26	0.03
Worms	0.23	0.25	0.47	0.56	0.06

*Loading Efficiency* mass of solubilized TAX/mass of initially added TAX

**Table IV.** Loading Efficiency of TAX into Worm-Like OCL3 Micelles at 5 and 10% (w/v)

	Total TAX Concentration (mg/ml)		
	2.5	5	10
5% Worm	0.44	0.49	0.17
10% Worm	0.64	0.59	0.18

*Loading Efficiency* mass of solubilized TAX/mass of initially added TAX

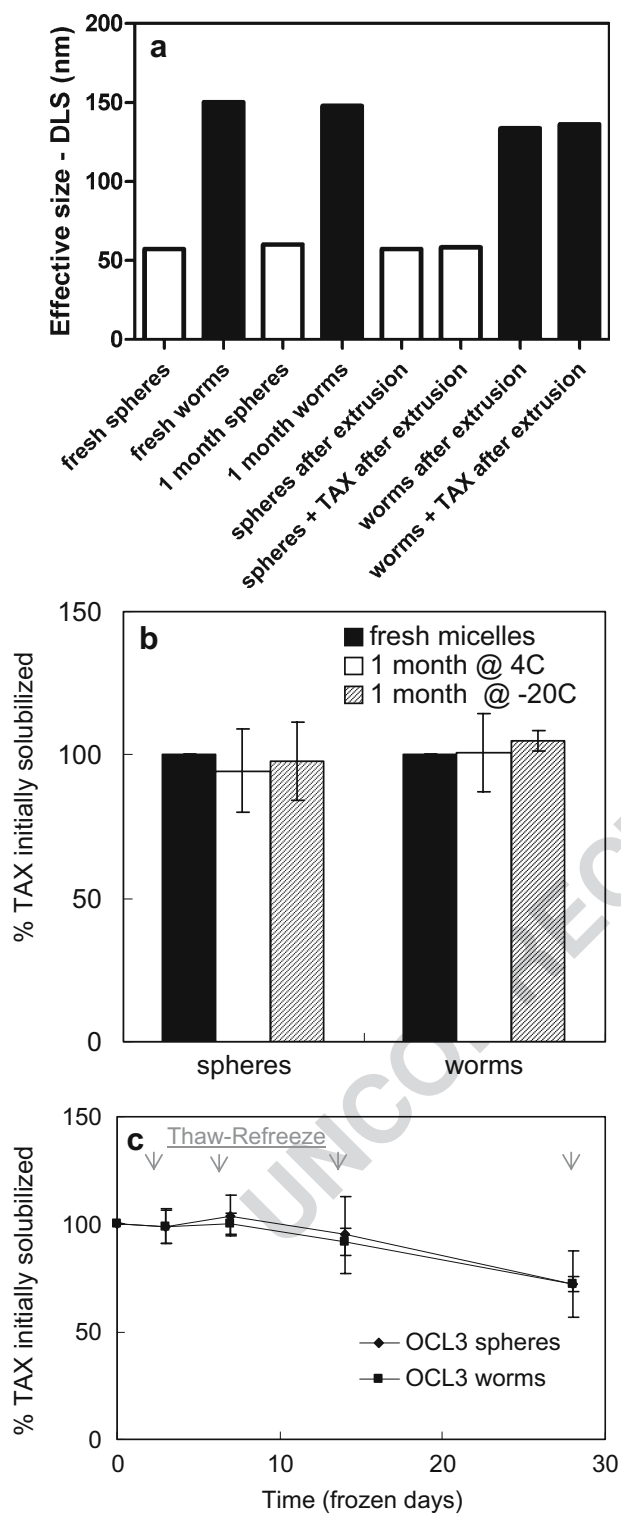


**Fig. 5.** Effect of extrusion, TAX loading, freeze–thawing and storage on micelle morphology and leakage of encapsulated drug. **a** Effect of extrusion, TAX loading and 1 month storage on the micelle effective size, determined by DLS; **b** effect of 1 month storage at 4 and  $-20^{\circ}\text{C}$  on TAX leakage from micelles; **c** effect of multiple freeze–thawing cycles at  $-20^{\circ}\text{C}$  on TAX leakage from micelles

that multiple freeze–thaw cycles lead to drug leakage from both morphologies. TAX-loaded OCL3 micelles were frozen at day 0, then thawed at day 3 for the test and re-frozen, which was repeated at day 7, 14, 28. By the fourth cycle, the TAX retained in the micelle cores decreased to about 70% of initial loading. The reasons are not yet as clear as the practical implications.

Release *in vitro* at  $37^{\circ}\text{C}$  was also studied at pH 7.4, per normal tissue pH, and also at pH 6.8 to mimic the slightly acidic cancerous tissue environment (29,35). As the PCL in OCL3 is known to undergo accelerated hydrolysis at acidic pH (30), TAX release rates proved to be 40% faster at lower pH but similar for both morphologies. This indicates that pH rather than shape is the more critical parameter to control drug release.

### Enhanced Cytotoxicity of TAX Released from OCL3 Micelles

Human lung carcinoma-derived A549 cells were used in cytotoxicity assays of both micelles as empty carriers and also as TAX-loaded carriers. The in-clinic, commercial TAX formulation with Cremophor EL was also included as a benchmark. Excipient toxicity is critically important to assessing the specific anticancer effect of TAX, and so for ease of comparison we therefore calculate the equivalent TAX concentration; for example, 0.8 mg TAX corresponds to about 1 g Cremophor EL (see “MATERIALS AND METHODS”). Based on such analyses, Cremophor EL shows a significant cytotoxic effect at only 2–3  $\mu\text{g}/\text{ml}$  equivalents of TAX (Fig. 6a). In contrast, the OCL3 polymeric micelles showed no obvious toxicity up to almost 100  $\mu\text{g}/\text{ml}$  TAX equivalents. Identifying the dose of excipients at which 80% of cells are still alive (‘inhibition constant’ IC80) as a parameterization of toxicity and then converting to cytotoxic carrier doses yields  $\text{IC80}_{\text{CremEL}}=120 \mu\text{g}/\text{ml}$  for Cremophor EL, which appears only slightly higher than  $\text{CMC}_{\text{CremEL}}\approx 90 \mu\text{g}/\text{ml}$  and implies the aggregate form of Cremophor EL is toxic (Fig. 6b). For both filomicelles and spheres,  $\text{IC80}_{\text{OCL3-micelle}}=1,500 \mu\text{g}/\text{ml}$ , which is about 13-orders of magnitude higher than  $\text{CMC}_{\text{OCL3}}$  and suggests mechanisms of cell death such as micellar poration previously discussed for PEO-PCL polymersomes (30). Regardless, the 13-fold difference indicates, of course, that OCL3 polymeric micelles are much safer excipients.

TAX formulations with the various carriers consistently improve cytotoxicity relative to delivery of free drug. While Fig. 6c shows that TAX-loaded Cremophor EL begins killing cells in the nanogram/milliliter range of TAX and kills nearly all cells at  $[\text{TAX}]\approx 10\text{--}100 \mu\text{g}/\text{ml}$  (Fig. 6a), the Cremophor EL excipient rather than TAX is clearly responsible for a significant fraction of the cytotoxicity. On the other hand, TAX-loaded OCL3 micelles exhibit similar cytotoxicity in the 10 ng/ml range, killing more than 35% A549 cancer cells. Importantly, the anticancer effects of TAX-loaded OCL3 micelles throughout the tested concentrations were all attributed to the drug activity, instead of the toxicity from the carriers. The fitted sigmoid dose–response curve showed that the  $\text{IC50}$ -cytotoxicity of TAX-loaded OCL3 micelles (at  $\sim 25 \text{ nM}$ ) was 13-fold more potent than free TAX (321 nM for A549 cells) and also 5-fold better than Cremophor EL TAX (Fig. 6d). Both worm-like filomicelles and spherical

relevant to storage. After a single cycle, there was no significant change in the length distribution shown in Fig. 1b or in TAX retention (Fig. 5c). However, the latter plot shows

444  
445  
446  
447  
448  
449  
450  
451  
452  
453  
454  
455  
456  
457  
458  
459  
460  
461  
462  
463  
464  
465  
466  
467  
468  
469  
470  
471  
472  
473  
474  
475  
476  
477  
478  
479  
480  
481  
482  
483  
484  
485  
486  
487  
488  
489  
490  
491  
492  
493  
494  
495  
496  
497  
498  
499  
500  
501  
502

**Micelles of Different Morphologies—Advantages of Worm-like Filomicelles of PEO-PCL in Paclitaxel Delivery**

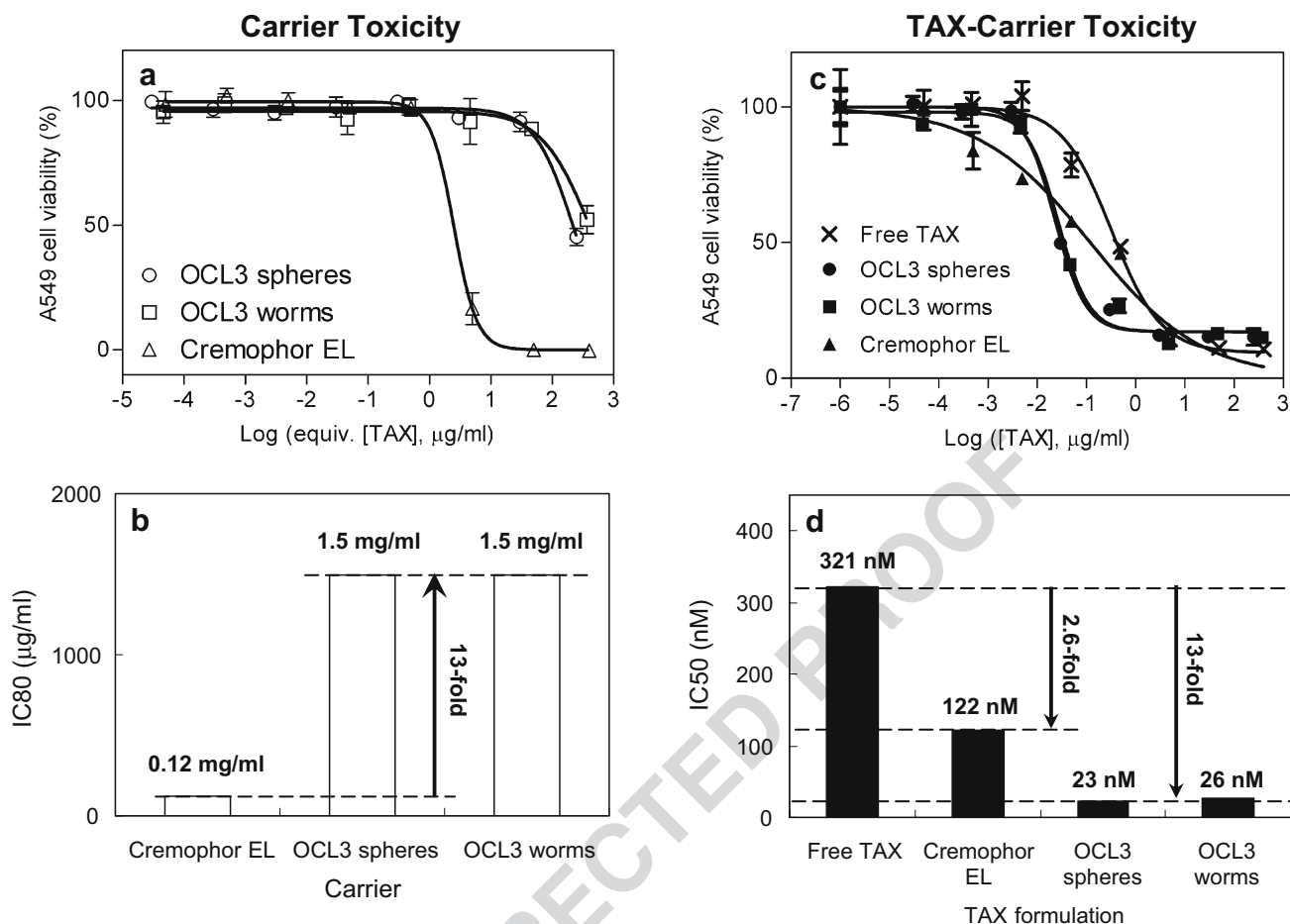


**Fig. 6.** Cytotoxicity study and IC<sub>50</sub> evaluation of TAX-loaded micelles on A549 human lung carcinoma cells. **a** Cytotoxicity of excipient only (OCL3 spheres, worms, and Cremophor EL) on A549 cells; **b** comparison of the excipient concentration at which 20% cells were killed (IC<sub>80</sub>); **c** cytotoxicity of different TAX formulations on A549 cells; **d** comparison of IC<sub>50</sub> of different TAX formulations. Sigmoid dose-responsive equation :  $Y = \text{Bottom} + (\text{Top} - \text{Bottom}) / (1 + 10^{((\text{LogIC}_{50} - X) * \text{HillSlope}))}$ , where  $X$  is the logarithm of TAX concentration,  $Y$  is the response and starts at bottom and goes to top, and HillSlope is the slope for the linear dropping region in the sigmoid curve

503 micelles showed the same enhanced cytotoxicity. Since OCL3  
 504 filomicelles have a higher drug loading capacity compared to  
 505 spherical micelles and otherwise display similar stability and  
 506 efficacy as spherical micelles, the filomicelles seem an attractive  
 507 alternative for the emerging tests of parenteral delivery (13).

508 **DISCUSSION**

509 TAX is a widely used chemotherapeutic for cancer  
 510 treatment, but its poor water solubility [0.3 μg/ml at 25°C  
 511 (18)] requires clinical use of solubilizers. Cremophor EL is  
 512 widely used but has side-effects and limitations that are clear  
 513 both in these simple studies and in the clinic. PEO-based  
 514 spherical micelles made from amphiphilic diblock copoly-  
 515 mers have been explored as an alternative type of carrier  
 516 system to load hydrophobic drugs and dyes into the  
 517 hydrophobic cores, and our recent studies have focused in  
 518 some detail on assembly and properties of worm-like  
 519 filomicelles (30–34). The needed copolymers are typically  
 520 composed of ~0.4–0.5 weight fraction of hydrophilic PEO  
 521 polymer and yield flexible but highly stable filamentous

micelles that surprisingly increase the circulation time in the  
 blood stream relative to spheres. Here we showed the  
 filomicelles -generally have a fluid core (Fig. 3), which favors  
 integration of drugs into their hydrophobic cores, and we  
 then examined the drug loading capacity and various other  
 performance aspects of PEO-PCL worm-like filomicelles for  
 comparison to spheres generated from the same filomicelles  
 by sonication. Loading advantages are clear (Fig. 4b,c,  
 Tables II, III, and IV), and some insight is gained from  
 simple calculations of volume to surface area for spheres and  
 cylinders. For spheres of radius  $r$ , volume/surface area =  
 $(4/3 \pi r^3) / (4\pi r^2) = r/3$ , whereas for cylinders of length  $L$ ,  
 volume/surface area =  $(\pi r^2 L) / (2\pi r L) = r/2$ . If micellar  
 area is thus held constant for a given mass of copolymer in  
 solution, then the filomicelles are expected to carry more  
 hydrophobic drug than spheres by a ratio of  $(r/2 - r/3) /$   
 $(r/3) = 50\%$ . The bigger difference of ~100% found here  
 certainly highlights the advantageous loading of drugs into  
 filomicelles. Furthermore, the maximum concentration of  
 solubilized TAX reached 3 mg/ml, placing filomicelles just  
 below Cremophor EL (marketed as formulations containing  
 6 mg/ml TAX) but among the top micelle-based TAX

544 delivery systems that usually enhance TAX solubility to 1–2  
545 mg/ml (18,21,23–25,42).

546 Although filomicelles appear novel and were perhaps  
547 even overlooked in past formulations that relied on sonica-  
548 tion, PEO-PCL block copolymer has been widely explored  
549 for drug delivery applications in the past. It consists of FDA-  
550 approved PEO plus the approved and degradable polyester  
551 PCL. We have previously found that hydrolytic degradation  
552 of PCL predominates at the distal hydroxyl-end such that the  
553 hydrophobic mass of PCL gradually decreases, increasing the  
554 weight fraction of PEO and converting the worm-like  
555 micelles towards spherical micelles (30). This process is  
556 greatly accelerated by low pH, which also accelerates release  
557 of TAX. On the other hand, degradation of PCL is  
558 significantly limited at low temperatures of 4 and –20°C,  
559 and the results here demonstrate stable storage of OCL3  
560 filomicelle morphologies at these low temperatures for  
561 a month (Fig. 5) without major complications from crystalliza-  
562 tion (Fig. 3). While multiple freeze–thaw cycles leads to loss  
563 of TAX for both worm-like and spherical micelles—as do  
564 other harsh conditions in extrusion, sonication, and lyophiliza-  
565 tion (not shown), only 1–2 cycles of freeze–thaw cycles  
566 have no obvious effect. Care should nonetheless be taken  
567 when preparing or storing TAX-loaded worm micelles.

568 Given the persistent circulation of filomicelles and  
569 minimal accumulation in rat lung (21), specific targeting of  
570 these novel morphologies to lung tumors should eventually  
571 provide a clear indication of directed drug delivery possibil-  
572 ities with filomicelles. Human lung cancer also continues to  
573 account for a significant of all cancer deaths. With these  
574 factors in mind as well as the intrinsic toxicity of Cremophor  
575 EL (Fig. 6a,b), we examined the *in vitro* delivery by  
576 filomicelles of TAX to A549 lung carcinoma cells, and we  
577 find that the spherical micelles and filomicelles are both 13-  
578 fold less toxic than Cremophor EL and, with loaded TAX,  
579 about 5-fold more effective in delivering a cytotoxic dose  
580 (Fig. 6c,d). Furthermore, since delivery of Cremophor EL is  
581 not pH-sensitive, such an *in vivo* formulation will tend to be  
582 less selective for tumors and further increase the risk of the  
583 excipient toxicity to normal cells.

584 **CONCLUSION**

585 Taken together, OCL3 based filomicelles appear to  
586 provide an excellent system for delivery of hydrophobic  
587 drugs, with enhanced drug solubility compared to spherical  
588 micelles but similar efficacy for a given dose of TAX.  
589 Morphological changes thus did not adversely impact drug  
590 release behavior and *in vitro* bioactivity. Future studies are  
591 likely to include conjugation with targeting moieties towards  
592 lung cancer cells and studies of *in vivo* tumor models with  
593 parenteral administration. Morphological effects under these  
594 more pathophysiological conditions clearly need to be  
595 mapped out.

596 **ACKNOWLEDGEMENTS**

597 This study was supported by grants from NIH-NIBIB  
598 and NSF-MRSEC.

**REFERENCES**

1. M. J. Vicent, R. Duncan. Polymer conjugates: nanosized 600  
medicines for treating cancer. *Trends Biotechnol.* **24**:39–47 601  
(2006). 602

2. A. Malugin, P. Kopeckova, and J. Kopecek. HEMA copolymer- 603  
bound doxorubicin induces apoptosis in ovarian carcinoma cells 604  
by the disruption of mitochondrial function. *Mol. Pharmacol.* 605  
**3**:351–361 (2006). 606

3. Y. Luo, M. R. Ziebell, and G. D. Prestwich. A hyaluronic acid- 607  
taxol antitumor bioconjugate targeted to cancer cells. *Bioma- 608*  
*cro-molecules.* **1**:208–218 (2000). 609

4. L. E. van Vlerkenand, and M. M. Amiji. Multi-functional 610  
polymeric nanoparticles for tumour-targeted drug delivery. 611  
*Expert Opin. Drug Deliv.* **3**:205–216 (2006). 612

5. B. Liu, S. Jiang, W. Zhang, F. Ye, Y. H. Wang, J. Wu, and D. Y. 613  
Zhang. Novel biodegradable HSAM nanoparticle for drug 614  
delivery. *Oncol. Rep.* **15**:957–961 (2006). 615

6. V. P. Torchilin. Recent advances with liposomes as pharmaceu- 616  
tical carriers. *Nat. Rev. Drug Discov.* **4**:145–160 (2005). 617

7. X. Guoand, F. C. Szoka Jr. Chemical approaches to triggerable 618  
lipid vesicles for drug and gene delivery. *Acc. Chem. Res* **36**:335– 619  
341 (2003). 620

8. F. Ahmed, R. I. Pakunlu, G. Srinivas, A. Brannan, F. Bates, M. L. 621  
Klein, T. Minko, and D. E. Discher. Shrinkage of a rapidly 622  
growing tumor by drug-loaded polymersomes: pH-triggered 623  
release through copolymer degradation. *Mol. Pharmacol.* **3**:340– 624  
350 (2006). 625

9. F. Ahmed, R. I. Pakunlu, A. Brannan, F. Bates, T. Minko, and 626  
D. E. Discher. Biodegradable polymersomes loaded with both 627  
paclitaxel and doxorubicin permeate and shrink tumors, inducing 628  
apoptosis in proportion to accumulated drug. *J. Control. Release.* 629  
**116**:150–158 (2006). 630

10. J. P. Xu, J. Ji, W. D. Chen, and J. C. Shen. Novel biomimetic 631  
polymersomes as polymer therapeutics for drug delivery. *J.* 632  
*Control. Release.* **107**:502–512 (2005). 633

11. Y. Bae, W. D. Jang, N. Nishiyama, S. Fukushima, and K. Kataoka. 634  
Multifunctional polymeric micelles with folate-mediated cancer 635  
cell targeting and pH-triggered drug releasing properties for 636  
active intracellular drug delivery. *Mol. BioSyst.* **1**:242–250 637  
(2005). 638

12. J. Wang, D. Mongayt, and V. P. Torchilin. Polymeric micelles 639  
for delivery of poorly soluble drugs: preparation and anticancer 640  
activity *in vitro* of paclitaxel incorporated into mixed micelles 641  
based on poly(ethylene glycol)–lipid conjugate and positively 642  
charged lipids. *J. Drug Target.* **13**:73–80 (2005). 643

13. Y. Geng, P. Dalhaimer, S. Cai, R. Tsai, M. Tewari, T. Minko, 644  
and D. E. Discher. Soft filaments circulate longer than spherical 645  
particles—shape effects in flow and drug delivery. *Nat. Nanotech.* 646  
(2007) (in press). 647

14. X. Tong, J. Zhou, and Y. Tan. Liquid chromatography/tandem 648  
triple-quadrupole mass spectrometry for determination of pac- 649  
litaxel in rat tissues. *Rapid Commun. Mass Spectrom.* **20**:1905– 650  
1912 (2006). 651

15. T. Y. Kim, D. W. Kim, J. Y. Chung, S. G. Shin, S. C. Kim, D. S. 652  
Heo, N. K. Kim, and Y. J. Bang. Phase I and pharmacokinetic 653  
study of Genexol-PM, a cremophor-free, polymeric micelle- 654  
formulated paclitaxel, in patients with advanced malignancies. 655  
*Clin. Cancer Res.* **10**:3708–3716 (2004). 656

16. S. C. Kim, J. Yu, J. W. Lee, E. S. Park, and S. C. Chi. Sensitive 657  
HPLC method for quantitation of paclitaxel (Genexol in biolog- 658  
ical samples with application to preclinical pharmacokinetics and 659  
biodistribution. *J. Pharm. Biomed. Anal.* **39**:170–176 (2005). 660

17. L. M. Han, J. Guo, L. J. Zhang, Q. S. Wang, and X. L. Fang. 661  
Pharmacokinetics and biodistribution of polymeric micelles of 662  
paclitaxel with Pluronic P123. *Acta Pharmacol. Sin.* **27**:747–753 663  
(2006). 664

18. O. Soga, C. F. van Nostrum, M. Fens, C. J. Rijcken, R. M. 665  
Schiffelers, G. Storm, and W. E. Hennink. Thermosensitive and 666  
biodegradable polymeric micelles for paclitaxel delivery. *J.* 667  
*Control. Release.* **103**:341–353 (2005). 668

19. R. T. Liggins, W. L. Hunter, and H. M. Burt. Solid-state 669  
characterization of paclitaxel. *J. Pharm. Sci.* **86**:1458–1463 (1997). 670

## Micelles of Different Morphologies—Advantages of Worm-like Filomicelles of PEO-PCL in Paclitaxel Delivery

- 671 20. S. C. Kim, D. W. Kim, Y. H. Shim, J. S. Bang, H. S. Oh, S. Wan  
672 Kim, and M. H. Seo. In vivo evaluation of polymeric micellar  
673 paclitaxel formulation: toxicity and efficacy. *J. Control. Release.*  
674 **72**:191–202 (2001).
- 675 21. S. Cheon Lee, C. Kim, I. Chan Kwon, H. Chung, and S. Young  
676 Jeong. Polymeric micelles of poly(2-ethyl-2-oxazoline)-block-  
677 poly(epsilon-caprolactone) copolymer as a carrier for paclitaxel.  
678 *J. Control. Release.* **89**:437–446 (2003).
- 679 22. T. Meyer, D. Waidelich, and A. W. Frahm. Separation and first  
680 structure elucidation of Cremophor EL-components by hyphen-  
681 ated capillary electrophoresis and delayed extraction-matrix  
682 assisted laser desorption/ionization-time of flight-mass spec-  
683 trometry. *Electrophoresis.* **23**:1053–1062 (2002).
- 684 23. Y. Moand, L.Y. Lim. Preparation and *in vitro* anticancer activity  
685 of wheat germ agglutinin (WGA)-conjugated PLGA nano-  
686 particles loaded with paclitaxel and isopropyl myristate. *J.*  
687 *Control. Release* **107**:30–42 (2005).
- 688 24. S. Q. Liu, Y. W. Tong, and Y. Y. Yang. Thermally sensitive micelles  
689 self-assembled from poly(*N*-isopropylacrylamide-co-*N,N*-dime-  
690 thylacrylamide)-*b*-poly(D,L-lactide-*c* *o*-glycolide) for controlled  
691 delivery of paclitaxel. *Mol. BioSyst.* **1**:158–165 (2005).
- 692 25. J. Xie, C. H. Wang. Self-assembled biodegradable nanoparticles  
693 developed by direct dialysis for the delivery of paclitaxel.  
694 *Pharm. Res.* **22**:2079–2090 (2005).
- 695 26. G. Gaucher, M. H. Dufresne, V. P. Sant, N. Kang, D. Maysinger,  
696 and J. C. Leroux. Block copolymer micelles: preparation,  
697 characterization and application in drug delivery. *J. Control.*  
698 *Release.* **109**:169–188 (2005).
- 699 27. F. Yoshii, D. Darwis, H. Mitomo, and K. Makuuchi. Cross-  
700 linking of poly(beta-caprolactone) by radiation technique and its  
701 biodegradability. *Radiat. Phys. Chem.* **57**:417–420 (2000).
- 702 28. R. T. Liggins, T. Cruz, W. Min, L. Liang, W. L. Hunter, and  
703 H. M. Burt. Intra-articular treatment of arthritis with micro-  
704 sphere formulations of paclitaxel: biocompatibility and efficacy  
705 determinations in rabbits. *Inflamm. Res.* **53**:363–372 (2004).
- 706 29. Z. G. Gao, D. H. Lee, D. I. Kim, and Y. H. Bae. Doxorubicin loaded  
707 pH-sensitive micelle targeting acidic extracellular pH of human  
708 ovarian A2780 tumor in mice. *J. Drug Target.* **13**:391–397 (2005).
- 709 30. Y. Gengand, D. E. Discher. Hydrolytic degradation of poly  
710 (ethylene oxide)-block-polycaprolactone worm micelles. *J. Am.*  
711 *Chem. Soc.* **127**:12780–12781 (2005).
- 712 31. P. Dalhaimer, F. S. Bates, and D. E. Discher. Single molecule  
visualization of stable, stiffness-tunable, flow-conforming worm  
micelles. *Macromolecules.* **36**:6873–6877 (2003).
32. Y. Kim, P. Dalhaimer, D. A. Christian, and D. E. Discher.  
Polymeric worm micelles as nano-carriers for drug delivery.  
*Nanotechnology.* **16**:S484–S491 (2005).
33. Y. Geng, F. Ahmed, N. Bhasin, and D. E. Discher. Visualizing  
worm micelle dynamics and phase transitions of a charged  
diblock copolymer in water. *J. Phys. Chem., B Condens. Mater.*  
*Surf. Interfaces Biophys.* **109**:3772–3779 (2005).
34. P. Dalhaimer, A. J. Engler, R. Parthasarathy, and D. E. Discher.  
Targeted worm micelles. *Biomacromolecules.* **5**:1714–1719 (2004).
35. S. D. Webb, J. A. Sherratt, and R. G. Fish. Alterations in  
proteolytic activity at low pH and its association with invasion: a  
theoretical model. *Clin. Exp. Metastasis.* **17**:397–407 (1999).
36. K. Vijayanand, D. E. Discher. Block copolymer worm micelles  
in dilution: mechanochemical metrics of robustness as a basis for  
novel linear assemblies. *J. Polym. Sci., B, Polym. Phys.* **44**:3431–  
3433 (2006).
37. L. Luo, J. Tam, D. Maysinger, and A. Eisenberg. Cellular  
internalization of poly(ethylene oxide)-*b*-poly(epsilon-caprolactone)  
diblock copolymer micelles. *Bioconjug. Chem.* **13**:1259–1265 (2002).
38. P. Skoglundand, A. Fransson. Continuous cooling and isother-  
mal crystallization of polycaprolactone. *J. Appl. Polym. Sci.*  
**61**:2455–2465 (1996).
39. V. Balsamo, C. U. de Navarro, and G. Gil. Microphase separation  
vs crystallization in polystyrene-*b*-polybutadiene-*b*-poly(epsilon-  
caprolactone) ABC triblock copolymers. *Macromolecules*  
**36**:4507–4514 (2003).
40. Y. Geng, D. E. Discher, J. Justynska, and H. Schlaad. Grafting  
short peptides onto polybutadiene-block-poly(ethylene oxide): a  
platform for self-assembling hybrid amphiphiles. *Angew. Chem.,*  
*Int. Ed. Engl.* **45**:7578–7581 (2006).
41. M. A. Hillmyerand, F. S. Bates. Synthesis and characterization  
of model polyalkane-poly(ethylene oxide) block copolymers.  
*Macromolecules* **29**:6994–7002 (1996).
42. J. H. Kim, K. Emoto, M. Lijima, Y. Nagasaki, T. Aoyagi, T. Okano,  
Y. Sakurai, and K. Kataoka. Core-stabilized polymeric micelle as  
potential drug carrier: increased solubilization of taxol. *Polym.*  
*Adv. Technol.* **10**:647–654 (1999).
43. G. L. Li and J. X. Tang. Diffusion of actin filaments within a thin  
layer between two walls. *Phys. Rev., E Stat. Nonlin. Soft Matter*  
*Phys.* **69**:(2004).

## AUTHOR QUERIES

### **AUTHOR PLEASE ANSWER ALL QUERIES.**

- Q1. Please check table header provided.
- Q2. Table 2 was split into Tables 2, 3, and 4, and citations 2 A-C were changed to Tables 2, 3, and 4. Please check if appropriate.
- Q3. Please provide bibliographic update for reference item [13] once available.

UNCORRECTED PROOF